

# Journal of Materials Chemistry A

Accepted Manuscript



This is an *Accepted Manuscript*, which has been through the Royal Society of Chemistry peer review process and has been accepted for publication.

*Accepted Manuscripts* are published online shortly after acceptance, before technical editing, formatting and proof reading. Using this free service, authors can make their results available to the community, in citable form, before we publish the edited article. We will replace this *Accepted Manuscript* with the edited and formatted *Advance Article* as soon as it is available.

You can find more information about *Accepted Manuscripts* in the [Information for Authors](#).

Please note that technical editing may introduce minor changes to the text and/or graphics, which may alter content. The journal's standard [Terms & Conditions](#) and the [Ethical guidelines](#) still apply. In no event shall the Royal Society of Chemistry be held responsible for any errors or omissions in this *Accepted Manuscript* or any consequences arising from the use of any information it contains.

## ARTICLE

# Preparation of Fine Particles of Scheelite-Monoclinic Phase $\text{BiVO}_4$ via an Aqueous Chelating Method for Efficient Photocatalytic Oxygen Evolution under Visible-light Irradiation

Cite this: DOI: 10.1039/x0xx00000x

Received 00th August 2014,  
Accepted 00th August 2014

DOI: 10.1039/x0xx00000x

[www.rsc.org/](http://www.rsc.org/)Sayuri Okunaka<sup>a,b</sup>, Hiromasa Tokudome<sup>a\*</sup>, Yutaka Hitomi<sup>c</sup> and Ryu Abe<sup>b\*</sup>

In this paper, we introduce a new synthetic method to prepare fine particles of  $\text{BiVO}_4$  with scheelite-monoclinic (s-m) phase, which is known as the most favorable crystal phase for photocatalytic water oxidation ( $\text{O}_2$  evolution) under visible light irradiation, based on a coordination chemistry approach in water. Stable aqueous solutions that contain both  $\text{Bi}^{3+}$  and  $\text{V}^{5+}$  complexes were prepared by simply mixing two aqueous solutions in which each cation was stabilized with an appropriate chelating agent. The use of chelating agents (glycolic acid (gly), L(+)-tartaric acid (tart), citric acid (cit), or ethylenediamine tetraacetic acid (edta)) was effective to form stable  $\text{V}^{5+}$  complexes from  $\text{NH}_4\text{VO}_3$ . On the other hand, only the use of two equivalents of edta with  $\text{Bi}(\text{NO}_3)_3 \cdot 5\text{H}_2\text{O}$  was effective to stabilize the  $\text{Bi}^{3+}$  complex in water, while the use of other ligands resulted in precipitations. Evaporation of the aqueous solution containing the stable  $\text{Bi}^{3+}$  and  $\text{V}^{5+}$  complexes and subsequent calcination in air at  $500^\circ\text{C}$  yielded s-m  $\text{BiVO}_4$  particles smaller than 300 nm, which were much smaller than  $\text{BiVO}_4$  particles prepared via conventional solid-state reactions (1–10  $\mu\text{m}$ ). In particular, the  $\text{BiVO}_4$  particles that were prepared with the tart ligand for  $\text{V}^{5+}$  stabilization possessed the smallest size (~80 nm) and exhibited the highest photocatalytic activity for  $\text{O}_2$  evolution from an aqueous solution containing an electron acceptor ( $\text{Ag}^+$  or  $\text{Fe}^{3+}$ ) under visible-light irradiation. These results strongly suggested that the tart ligand effectively suppresses particle growth during the crystallization process and thereby affords small  $\text{BiVO}_4$  particles with high crystallinity, both of which are necessary to achieve highly efficient photocatalysis.

## Introduction

Photocatalytic splitting of water is a promising technology for the clean and direct production of  $\text{H}_2$  from water, and thus is expected to contribute to the realization of a sustainable society based on clean energy cycles involving  $\text{H}_2$  carriers. Great progress has been made on photocatalytic (and photoelectrochemical) water splitting<sup>1–6</sup> since the pioneering work on photoelectrochemical water splitting using  $\text{TiO}_2$  anodes first reported in 1972.<sup>7</sup> Development of photocatalysis systems that efficiently split water by harvesting a wide range of visible light is crucial to demonstrate the feasibility of photocatalytic solar  $\text{H}_2$  production. Photocatalytic water splitting under visible light has been demonstrated on two different systems, i.e., one-step<sup>8–11</sup> and two-steps systems.<sup>12,13</sup> The latter system (so-called Z-scheme) basically consists of two different photocatalysts and a redox couple (e.g.,  $\text{IO}_3^-/\Gamma^-$ ) that mediates the electron transfer between them.<sup>14,15</sup> Among the

various visible-light-responsive photocatalysts developed so far, bismuth vanadate ( $\text{BiVO}_4$ ) has attracted much attention as an efficient photocatalyst for  $\text{O}_2$  evolution under visible-light irradiation in the presence of various reversible electron acceptors, such as  $\text{Fe}^{3+}/\text{Fe}^{2+}$ ,  $[\text{Co}(\text{bpy})_3]^{3+/2+}$ , and  $[\text{Co}(\text{phen})_3]^{3+/2+}$ .<sup>16–20</sup> The main crystal forms of  $\text{BiVO}_4$  are zircon-tetragonal (z-t), scheelite-monoclinic (s-m) and scheelite-tetragonal (s-t).<sup>21</sup> A number of reports have demonstrated that s-m phase  $\text{BiVO}_4$  particles exhibit higher photocatalytic activity for  $\text{O}_2$  evolution than that of other crystal phases.<sup>22,23</sup> The higher activity of s-m  $\text{BiVO}_4$  is primarily because it has a narrower bandgap (2.4 eV) than the others, which is due to the contribution of Bi-6s orbitals mixed with O-2p orbitals in its valence band. However, it is widely recognized that the activity of photocatalysts is determined not only by the band structure but also by other physicochemical properties of the semiconductor particles.<sup>24</sup> Among these

physicochemical properties, the particle size often influences the photocatalytic activity significantly, because it dictates the distance of charge transport from the bulk material to its surface, and the number of active sites on the surface. This influence differs depending on the reaction systems.<sup>24</sup> Thus, various methods, such as solid-state reactions,<sup>25-27</sup> liquid-phase reactions,<sup>28,29</sup> hydrothermal processes,<sup>30-33</sup> and co-precipitation techniques,<sup>34</sup> have been employed to control the crystal phase and particle size of BiVO<sub>4</sub> photocatalysts in order to achieve highly efficient O<sub>2</sub> evolution. However, the synthesis of small s-m phase BiVO<sub>4</sub> particles is basically difficult because the s-m phase is formed at high temperatures. For example, it has been reported that the phase transition from z-t to s-m phase occurs above 500 °C in conventional solid-state reactions. Such high temperatures usually cause crystal growth and aggregation. Although the application of liquid-base methods, such as hydrothermal processes and co-precipitation methods, allow the formation of s-m phase BiVO<sub>4</sub> at low temperatures, there is still a limited number of reports on the preparation of fine s-m BiVO<sub>4</sub> particles smaller than 100 nm in diameter.<sup>33,34</sup> In addition, the low crystallinity of s-m BiVO<sub>4</sub> particles prepared *via* such methods generally necessitates post-calcination in order to improve their activity by reducing crystal defects where the recombination of photoexcited electrons and holes is often accelerated. However, such post-calcination inevitably leads to particle growth.

We have recently demonstrated the synthesis of fine particles (ca. 50 nm) of Rh-doped SrTiO<sub>3</sub> (SrTiO<sub>3</sub>:Rh) *via* an environmentally friendly water-based process, and their high activity for photocatalytic H<sub>2</sub> evolution under visible light.<sup>35</sup> One of the key features of this process was the use of an appropriate combination of chelating agents, which effectively stabilized the titania nanocolloid (ca. 4 nm) precursor, even in water.<sup>36</sup> The calcination of the precursor sols produced highly crystallized SrTiO<sub>3</sub>:Rh with particles sizes of ca. 50 nm, even after calcination above 900 °C. These results suggested that appropriate chelators not only stabilize precursor cations in water but also suppressed particle growth during calcination, affording highly crystallized and small particles of mixed metal oxides.

In this study, we attempt to synthesize fine particles of s-m phase BiVO<sub>4</sub> in aqueous solution through a similar chelating process. Various chelating ligands with different numbers of carboxyl groups are used to stabilize the Bi<sup>3+</sup> and V<sup>5+</sup> ions in aqueous solution. The influence of these ligands on the size and photocatalytic activity of the obtained s-m BiVO<sub>4</sub> particles is evaluated.

## Experimental

### Materials

Ammonium vanadate(V) (99%, NH<sub>4</sub>VO<sub>3</sub>), bismuth(III) nitrate pentahydrate (99.9%, Bi(NO<sub>3</sub>)<sub>3</sub>·5H<sub>2</sub>O), glycolic acid (gly), L(+)-tartaric acid (tart), citric acid (cit), ethylenediamine tetraacetic acid (edta), silver nitrate (99.5%, AgNO<sub>3</sub>) and

iron(III) chloride (99.9%, FeCl<sub>3</sub>·6H<sub>2</sub>O) were purchased from Wako Pure Chemical Industries Ltd., Japan. Aqueous ammonia (28.0-30.0%) was purchased from Kanto Chemical Ltd., Japan. All reagents were used as received, and all the experiments were carried out under ambient conditions without eliminating the moisture from the atmosphere.

### Preparation of fine BiVO<sub>4</sub> particles *via* an aqueous chelating method

BiVO<sub>4</sub> particles were prepared *via* a newly developed aqueous chelating method (hereafter denoted by AC-method). Bi(NO<sub>3</sub>)<sub>3</sub>·5H<sub>2</sub>O (0.17 mol/L, 0.82 g) was added to an aqueous solution (10 mL) containing edta (0.34 mol/L, 0.73 g) and aqueous ammonia (ca. 1.0 mL) to adjust the pH of the solution to 8, producing a clear solution (hereafter denoted by Bi(edta)-sol.). For the chelation of V<sup>5+</sup> species, four kinds of ligands (gly, tart, cit, or edta) were tested. NH<sub>4</sub>VO<sub>3</sub> (0.17 mol/L, 0.20 g) was added to an aqueous solution (10 mL) containing one of the ligands (0.17 mol/L). Then, aqueous ammonia (ca. 0.5 mL) was added, resulting in a transparent solution of pH 7-8, depending on the ligand (hereafter denoted by V(L)-sol., where L = gly, tart, cit, or edta). The Bi(edta)-sol. and one of the V(L)-sol. were mixed at a molar ratio of Bi:V = 1:1 with stirring (30-60 min) at room temperature to prepare the precursor solutions for BiVO<sub>4</sub> synthesis (hereafter denoted by Bi(edta)+V(L)-sol., where L = gly, tart, cit, or edta). The precursor solution was evaporated at ca. 80 °C to complete dryness, followed by calcination in air. To determine the appropriate calcination temperature, thermal analysis (TG-DTA, TG-8120, Rigaku) was carried out for the precursor gels (10 mg) obtained by the drying of the Bi(edta)+V(L)-sol.. No significant weight loss was observed above 430 °C for all samples (see Fig. S1), strongly suggesting that almost all ligands were combusted at ca. 430 °C. Thus, we set the basic calcination temperature as 500 °C, while other temperatures (e.g., 450 and 550 °C) were applied in some cases. The samples calcined at 500 °C are denoted by AC-L (where L = gly, tart, cit, or edta), unless otherwise stated. For comparison, BiVO<sub>4</sub> particles were prepared *via* the conventional solid-solution reaction method (SS-method) using NH<sub>4</sub>VO<sub>3</sub> and Bi(NO<sub>3</sub>)<sub>3</sub>·5H<sub>2</sub>O as metal sources. These materials were mixed at a molar ratio of Bi:V = 1:1 and calcined in air at 500-700 °C for 6 h, yielding BiVO<sub>4</sub> particles, hereafter denoted by SS-T (where T is the calcination temperature).

### Characterization

<sup>1</sup>H NMR spectra of the precursor solutions were recorded in 10% D<sub>2</sub>O on a JMN-ECA 500 spectrometer (JEOL). For <sup>1</sup>H NMR measurements, sodium 3-(trimethylsilyl)propionate-2,2,3,3-d<sub>4</sub> in D<sub>2</sub>O was used as an external reference in a capillary tube.

The obtained powdered samples were characterized by X-ray diffraction (XRD, PANalytical, X'Pert Pro, rotating anode diffractometer, 45 kV, 40 mA) with Cu K $\alpha$  radiation ( $\lambda_{K\alpha}$  = 1.5406 Å), ultraviolet-visible-near infrared spectrometry (UV-Vis-NIR, DRS, Jasco, V-670), and scanning electron

microscopy (SEM, HITACHI, S-4100). Specific surface areas of the powdered samples were determined by N<sub>2</sub> adsorption at 77 K (BET, MicrotracBEL, BELSORP mini).

### Photocatalytic reactions

The photocatalytic activity of the BiVO<sub>4</sub> particles was evaluated by monitoring O<sub>2</sub> evolution from an aqueous solution containing an electron acceptor (Ag<sup>+</sup> or Fe<sup>3+</sup>) under visible-light irradiation, using a gas-closed circulation system equipped with a top-irradiation type reaction cell (Pyrex-made). The catalyst powder (50 mg) was suspended in 120 mL of an aqueous AgNO<sub>3</sub> solution (10 mM, pH 5.2) or an aqueous FeCl<sub>3</sub> solution (10 mM, pH 2.2). The suspension was thoroughly degassed *via* repeated evacuation with a vacuum pump, and subsequently introduction of Ar gas (80 Torr). Light irradiation was introduced from the top of the reactor with a 300 W Xe-arc lamp (Perkin-Elmer, Cermax PE300BF) attached with a cut-off filter (Hoya; L42) to eliminate the UV light. The gases in the circulation system were analyzed and quantified by means of an on-line gas chromatograph (GL Science; GC-3200, TCD, Ar carrier, MS-5A column).

## Results and discussion

### Preparation of stable BiVO<sub>4</sub> precursor solutions with different ligands

In the present study, we attempted to stabilize V<sup>5+</sup> and Bi<sup>3+</sup> cations in water using four different ligands (gly, tart, cit, or edta), and the results are summarized in Table S1. The simple addition of Bi(NO<sub>3</sub>)<sub>3</sub>·5H<sub>2</sub>O or NH<sub>4</sub>VO<sub>3</sub> to water results in a precipitation due to rapid hydrolysis (Fig. S2 (a)–(b)). In contrast, the combination of Bi(NO<sub>3</sub>)<sub>3</sub>·5H<sub>2</sub>O with two equivalents of edta produces a transparent solution without any precipitation (see Fig. S2 (c)), whereas the use of other ligands, even two equivalents, results in precipitation. The solution prepared with two equivalents of edta will be denoted by Bi(edta)-sol., hereafter. For NH<sub>4</sub>VO<sub>3</sub>, all the ligands (L = gly, tart, cit, or edta) were effective in stabilizing V<sup>5+</sup>, even at just one equivalent (see Fig. S2 (d)). These solutions prepared with one equivalent of ligand will be denoted by V(L)-sol. (where L = gly, tart, cit, or edta) hereafter. Although the formation of

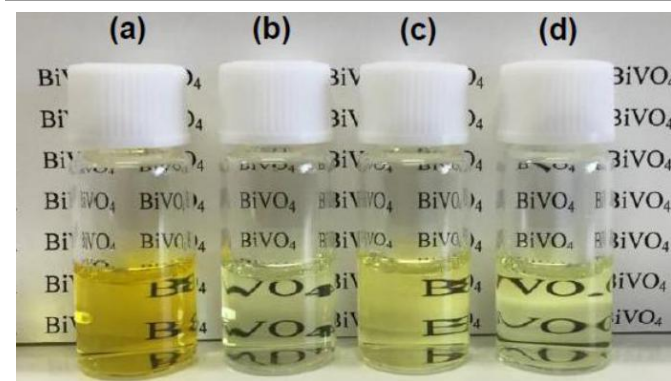


Fig. 1 A photograph of aqueous solutions obtained by mixing Bi(edta)-sol. and V(L)-sol (L = (a) gly, (b) tart, (c) cit, and (d) edta).

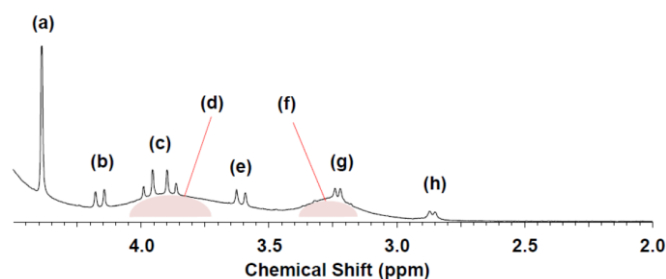


Fig. 2 <sup>1</sup>H NMR spectrum of aqueous solution of Bi(edta)-sol. mixed with V(tart)-sol. (Bi(edta)+V(tart)-sol.).

stable complexes of V<sup>5+</sup> and Bi<sup>3+</sup> in aqueous solution have been reported previously,<sup>37–47</sup> excess amounts of ligand were used in most cases. In the present case, it is confirmed that one and two equivalents of the appropriate ligand are effective for stabilization of V and Bi cations, respectively. As for the stabilization of Bi<sup>3+</sup> cation, less amounts (e.g., one and a half equivalents) of edta results in precipitation (as summarized in Table S1). In addition, NMR spectrum of Bi(edta)-sol. indicates that there is no signals corresponding to free edta species in the solution. These results strongly suggest that more than one edta ligands contribute to the stabilization of one Bi<sup>3+</sup> cation. It is also confirmed that the simple mixing of Bi(edta)-sol. with V(L)-sol. (L = tart, cit, or edta) produces clear yellow solutions (see Fig. 1). Although the combination of Bi(edta)-sol. and V(gly)-sol. produces a clear yellow solution immediately after mixing, precipitates are gradually generated. The other mixed solutions show high stability and do not produce any appreciable precipitations, even after leaving under atmospheric conditions for more than one year. As will be discussed later, the kind of ligands used for V<sup>5+</sup> stabilization significantly influences the size and activity of the BiVO<sub>4</sub> particles produced after calcination of the mixed solutions (Bi(edta)+V(L)-sol.). Particularly, the use of tart ligands with V<sup>5+</sup> (V(tart)-sol.) produces significantly smaller BiVO<sub>4</sub> particles, suggesting that the presence of the V<sup>5+</sup> species coordinated by tart ligands (V(tart) species) in the mixed solution plays a significant role in reducing the particle size. However, the possibility of replacement of the tart that originally coordinated to V<sup>5+</sup> by the edta that originally coordinated to Bi<sup>3+</sup>, possibly by the residual free edta, in the mixed solution cannot be excluded. Thus, liquid state <sup>1</sup>H NMR measurements were conducted to obtain detailed information on the species in Bi(edta)+V(tart)-sol., and the spectrum is shown in Fig. 2. The assignments of the observed signals estimated from comparison with authentic samples are summarized in Table S2. The spectrum exhibits signals assignable to both the edta that coordinates to Bi<sup>3+</sup> at 3.90 and 3.25 ppm (Fig. 2 (a)–(b)) and the edta that coordinates to V<sup>5+</sup> at 4.15, 3.90, 3.60, 3.20, and 2.85 ppm (Fig. 2 (c)–(g)). These results indicate that a some of the tart ligands that originally coordinated to the V<sup>5+</sup> cation are replaced by edta ligands in the mixed solution. However, it is difficult to confirm the presence of tart ligands that still coordinate to V<sup>5+</sup> cation (V-tart) after mixing due to the overlap of the V-tart and free

tart signals (at 4.3 ppm, Fig. 2 (f)). The line width of the singlet signal at 4.3 ppm (a) is broader (5.6 Hz) than that of the free tart molecules (0.7 Hz) but narrower than that of the pure V(tart) complex (7.3 Hz). These findings strongly suggest that some of the tart ligands originally coordinated to  $V^{5+}$  are replaced by the excess edta ligands after mixing. However, titration experiments with excess of edta (up to three equivalents, see the detail in SI) indicate that the V-tart complex can exist to some extent in the solution even when it contains two equivalents of free edta, strongly suggesting that complete replacement of the original tart ligands by edta does not occur under the present conditions. Based on these results, we conclude that Bi(edta)+V(tart)-sol. contains mainly V(tart) and Bi(edta), along with free tart, and V(edta) to some extent.

### Characterization of the $BiVO_4$ fine particles prepared via the aqueous chelating method

Figure 3 shows a photograph of the AC-L samples, which were obtained by drying the precursor solution (Bi(edta)+V(L)-sol.) followed by calcination at 500 °C in air. The volumes of the samples increase after calcination, regardless of the stabilizing ligands. In particular, the AC-tart sample shows the most significant increase in volume compared with the other AC-L samples.

The XRD patterns of  $BiVO_4$  particles prepared via the AC-method are shown in Fig. 4. Doublet peaks at ca. 18.5° and 35° are observed for the  $BiVO_4$  particles prepared with three ligands (tart, cit, and edta), indicating the production of single-phase s-m  $BiVO_4$ .<sup>22,29</sup> Conversely, the  $BiVO_4$  particles prepared with gly ligands (AC-gly) show a single broad peak at ca. 18.5°, implying the formation of s-m  $BiVO_4$  with low crystallinity and/or the co-existence of s-t  $BiVO_4$ .<sup>29,48</sup> The band gap of the AC-gly sample (see Table 1) estimated from the UV-spectrum (see Fig. S3) is ca. 2.4 eV, which is characteristic of s-m phase  $BiVO_4$ .<sup>22,23</sup> The same value (2.4 eV) is obtained with other preparations, i.e., AC-tart, AC-cit, and AC-edta. The V-O bond length (ca. 1.69 Å), calculated from the corresponding Raman stretching signal at around 830  $cm^{-1}$  for the AC-gly samples, is almost the same as the values for other samples, such as AC-tart, as seen in Table 1. This value agrees well with the reported



Fig. 3 Photographs of the dried gel obtained by dryness of the Bi(edta)+V(tart)-sol. and the AC-L samples obtained by dryness of the precursor solution Bi(edta)+V(L)-sol. (L = (a) gly, (b) tart, (c) cit or (d) edta) followed by calcination at 500°C in air.

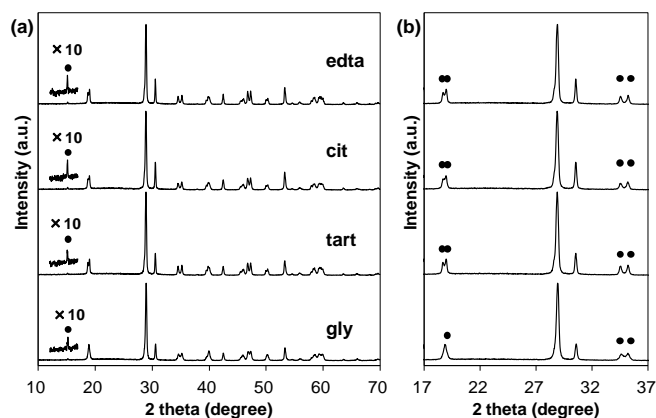


Fig. 4. XRD patterns of  $BiVO_4$  particles prepared via AC-method with different ligands (gly, tart, cit or edta) followed by calcination at 500°C in air.

Table 1. Stretching Raman shift of V-O bond and bond length of V-O on  $BiVO_4$  particles prepared via AC method with different ligands (gly, tart, cit or edta) followed by calcination at 500°C in air.

	B.G. [eV]	Stretching Raman shift V-O bond [ $cm^{-1}$ ]	Bond length V-O [Å] <sup>a</sup>
AC-gly	2.4	825	1.697
AC-tart	2.4	827	1.695
AC-cit	2.4	828	1.695
AC-edta	2.4	828	1.695

<sup>a</sup>calculated using the empirical expression:  $\nu (cm^{-1}) = 21349 \exp[-1.9176 R(\text{Å})]$

value for s-m  $BiVO_4$  (1.69 Å) but is appreciably different from that for s-t  $BiVO_4$  (1.72 Å).<sup>26,49</sup> From these results, we can conclude that the AC-gly sample predominantly consists of s-m  $BiVO_4$  with low crystallinity. The XRD patterns of the  $BiVO_4$  particles prepared via the SS-method with calcination in air at 600 and 700 °C (SS-600 and 700) also indicate single-phase s-m  $BiVO_4$ , whereas an unknown peak is observed in the sample calcined at 500 °C (SS-500, see Fig. S4).

Figure 5 shows SEM images of the  $BiVO_4$  samples. The primary particle sizes in the AC-samples calcined at 500 °C range from 80 to 300 nm, which are much smaller than those of the SS-samples (1–10 μm) containing single-phase s-m material (SS-600, SS-700). Specifically, the sample prepared with the tart ligand (AC-tart) contains the smallest particles (ca. 80 nm) with relatively homogeneous distribution. In addition, the specific surface area of AC-tart (5.2  $m^2 g^{-1}$ ) is larger than those of other samples (see the bottom left in Fig. 5 for each sample). Since all the AC-samples were prepared under the same conditions (i.e., pH of precursor solution, concentration of metal ions, calcination temperature, etc.) except for the ligands used, the significant difference in the particle size strongly suggests that the ligand used for stabilizing the  $V^{5+}$  ions is the key factor in determining the particle size after calcination. During the drying and calcination of the Bi(edta)+V(L)-sol. in the AC-method, the polymerization reaction first proceeds between the functional groups (i.e., -COOH and -OH) of the

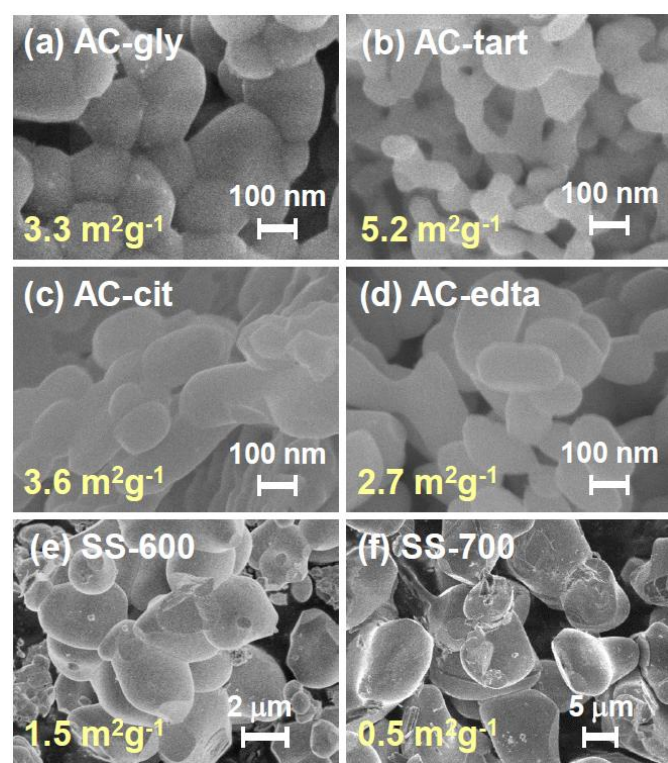


Fig. 5 SEM images of  $\text{BiVO}_4$  particles prepared *via* AC- and SS-methods followed by calcinations with different temperatures ((a)AC-gly, (b) AC-tart, (c) AC-cit, (d) AC-edta, (e) SS-600 and (f) SS-700).

ligands, followed by nuclei generation (i.e., crystallization) and further crystal growth. The TG-DTA data (see Fig. S1) strongly suggest that the organic compounds in the dried gels are completely combusted at ca. 430 °C, regardless of the type of ligands used for stabilizing the  $\text{V}^{5+}$  ion. As shown in Fig. S5, the particle size of AC-tart calcined at 450 °C is slightly smaller than that when it is calcined at 500 °C. Similarly, the particle size of the AC-samples prepared using other ligands and calcination at 450 °C is slightly smaller than that of those prepared at 500 °C. These findings indicate that the particle size of each AC-sample is predominantly determined by the processes occurring below ca. 450 °C, not those above 450 °C. At temperatures lower than 430 °C, at which organic species still remain, processes such as polymerization, nuclei generation, and crystal growth occur. In general, the number of carboxyl groups in the ligands considerably influences nuclei generation.<sup>50</sup> A higher number of carboxyl groups in the ligands generally causes the formation of larger nuclei due to the increased probability of polymerization. Therefore, the AC-samples prepared with cit and edta, which have three and four carboxyl groups, respectively, formed larger nuclei in the precursor during polymerization, thereby resulting in the production of  $\text{BiVO}_4$  particles with large sizes (> 100 nm) after calcination. Although the number of carboxyl groups in gly is lower than that in tart, the size of  $\text{BiVO}_4$  particles prepared with gly (AC-gly) is larger (100–300 nm) than that prepared with tart (ca. 80 nm). This contradicting phenomenon is explained by the instability of the precursor solution. As described in the

previous section, the precursor solution prepared using the gly ligand for  $\text{V}^{5+}$  stabilization ( $\text{Bi}(\text{edta})+\text{V}(\text{gly})\text{-sol.}$ ) is unstable and gradually produces precipitations, indicating that the hydrolysis of  $\text{V}^{5+}$  species proceeds *via* replacement of gly ligands with water molecules. Thereby, larger and inhomogeneous nuclei are produced during the drying of  $\text{Bi}(\text{edta})+\text{V}(\text{gly})\text{-sol.}$ , affording larger particles after calcination. Another possibility will be the difference in combustion heat of each chelating ligands during the calcinations process. The enthalpy of combustion of each ligand molecule increases with the increasing numbers of carboxyl group (gly: -697.23, tart: -1159.3, cit: -1960.6, edta: -4458.1 kJ/mol). The higher heat released during the combustion of ligands with higher numbers of carboxyl groups possibly accelerate the particle growth, resulting in the production of larger particles.

#### Photocatalytic $\text{O}_2$ evolution on $\text{BiVO}_4$ prepared *via* aqueous chelating method

The photocatalytic activity of the  $\text{BiVO}_4$  samples was evaluated for  $\text{O}_2$  evolution from an aqueous solution containing an electron acceptor ( $\text{Ag}^+$  or  $\text{Fe}^{3+}$ ) under visible-light irradiation ( $\lambda > 410 \text{ nm}$ ). The initial rates of  $\text{O}_2$  evolution over AC- and SS-samples are summarized in Table 2. The rate of  $\text{O}_2$  evolution over the AC-samples was dependent on the calcination temperature during the preparation process. The highest rate is observed for AC-sample calcined at 500 °C. For the SS-samples, the optimum calcination temperature is 600 °C.

Figure 6 shows the time course of  $\text{O}_2$  evolution from aqueous solution over these samples under visible-light irradiation in the presence of an electron acceptor ( $\text{Ag}^+$  or  $\text{Fe}^{3+}$ ). It is known that  $\text{Ag}^+$  is irreversibly reduced by photoexcited electrons; producing stable Ag metal on the surface of photocatalyst. Thus,  $\text{Ag}^+$  is often used for the feasibility test whether a certain photocatalyst satisfies the thermodynamic and kinetic potentials for  $\text{O}_2$  evolution. On the other hand, the photocatalytic  $\text{O}_2$  evolution with  $\text{Fe}^{3+}$  electron acceptor is basically more difficult to be achieved because the backward reaction, i.e., re-oxidation of the produced  $\text{Fe}^{2+}$ , is readily occurred in most cases. However, successful  $\text{O}_2$  evolution with  $\text{Fe}^{3+}$  acceptor, accompanied by stoichiometric generation of  $\text{Fe}^{2+}$ , indicates the possibility of Z-scheme water splitting when coupled with an appropriate  $\text{H}_2$ -evolving photocatalyst. Although largely steady rates of  $\text{O}_2$  evolution are observed for all the cases in the initial period of photo-irradiation, the rates gradually decrease due to the occurrence of the backward reaction (i.e., re-oxidation of  $\text{Fe}^{2+}$  by holes) or deposition of Ag metal particles on the surface. No significant change was observed in the particles size and XRD pattern of the AC-tart samples after  $\text{O}_2$  evolution reaction as seen in Fig. S5 and S6, respectively, strongly suggesting that the present AC-tart sample are stable for photocatalytic water oxidation. The higher activity over the AC-tart sample calcined at 500 °C than that prepared at 450 °C is certainly due to the improved crystallinity of the particles, which leads to a decreased amount of crystal defects that function as recombination sites between photogenerated electrons and holes. The appreciable decrease in efficiency of the AC-

Table 2. Photocatalytic O<sub>2</sub> evolution from an aqueous solution containing electron acceptor under visible light irradiation on BiVO<sub>4</sub> samples that were prepared under different conditions.<sup>a</sup>

	Calcination temperature [°C]	O <sub>2</sub> evolution rate [μmol h <sup>-1</sup> ]	
		Ag <sup>+</sup>	Fe <sup>3+</sup>
AC-gly	500	8	40
AC-tart	450	13	59
AC-tart	500	16	90
AC-tart	550	15	81
AC-cit	500	11	44
AC-edta	500	10	41
SS	500	4	16
SS	600	6	19
SS	700	3	16

<sup>a</sup>Catalyst, 0.05 g; reactant solution, 120 mL of 10 mM aqueous solution containing an electron acceptor (Ag<sup>+</sup> or Fe<sup>3+</sup>); light source, 300 W Xe lamp with cut-off filters (λ > 410 nm).

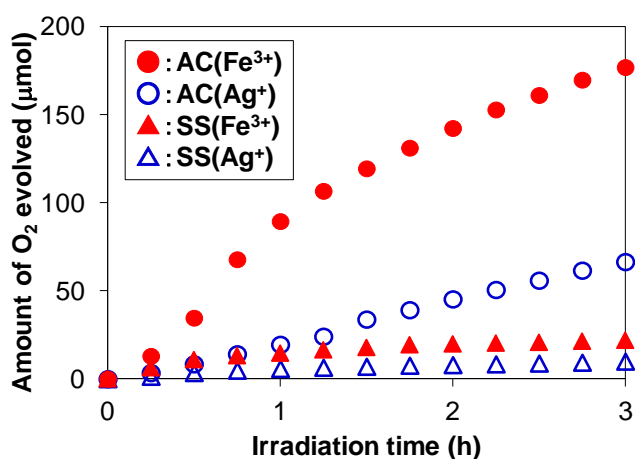


Fig. 6 O<sub>2</sub> evolution from an aqueous solution containing an electron acceptor (Ag<sup>+</sup> or Fe<sup>3+</sup>) under visible-light irradiation over BiVO<sub>4</sub> photocatalyst prepared *via* AC- or SS-method followed by calcination (AC-tart and SS-600). Conditions: Catalyst, 0.05 g; reactant solution, 120 mL of 10 mM aqueous solution containing an electron acceptor (Ag<sup>+</sup> or Fe<sup>3+</sup>); light source, 300 W Xe lamp with cut-off filters (λ > 410 nm).

samples calcined above 550 °C can be explained by the increase in particle size (see Fig. S7), which increases the migration distance for charge carriers generated in the bulk material, and consequently increases the possibility of their recombination before reaching the surface. The rate of O<sub>2</sub> evolution over the AC-samples also changes depending on the type of ligand used for V<sup>5+</sup> stabilization in the precursor solution, with the rate increasing in the order AC-gly < AC-edta < AC-cit < AC-tart, when compared at the same calcination temperature (500 °C). The primary particle size of AC-tart (80 nm) is much smaller than that of the AC-samples prepared with other ligands (gly, cit, and edta) (100–300 nm) (see Fig. 5). The O<sub>2</sub> evolution rate over AC-gly is lower than that over AC-edta, despite the larger specific surface area of AC-gly. This lower activity may be explained by the lower crystallinity of the AC-gly particles, as confirmed by XRD measurements. Thus, the highest O<sub>2</sub> evolution rate for AC-tart can be explained by it having the smallest particle size with similar crystallinity among the samples, except for AC-gly. It is also confirmed that

the BiVO<sub>4</sub> particles prepared *via* the AC-method show higher activity for O<sub>2</sub> generation than the BiVO<sub>4</sub> samples prepared *via* the conventional SS-method. The O<sub>2</sub> evolution rate with AC-tart is ca. three times higher than that with SS-600. In addition, the quantum efficiencies on AC-tart were determined to be 1.2% and 0.86% for Fe<sup>3+</sup> and Ag<sup>+</sup>, respectively. These values are higher than those obtained for the SS-600 (0.53% and 0.3% for Fe<sup>3+</sup> and Ag<sup>+</sup>, respectively). These results indicate that the present AC-method is extremely useful for the preparation of fine s-m BiVO<sub>4</sub> particles that exhibit high activity for photocatalytic O<sub>2</sub> evolution from water under visible-light irradiation.

## Conclusions

In the present study, we successfully synthesized fine particles of s-m BiVO<sub>4</sub> (80–300 nm) with a particle size smaller than those produced with conventional solid-state reactions (1–10 μm) *via* a newly developed aqueous chelating method. The kind of ligands used for the stabilization of V<sup>5+</sup> ions in the precursor solution was found to significantly influence the particle size of the obtained BiVO<sub>4</sub>. Among the ligands examined, the use of the tart ligand produced s-m BiVO<sub>4</sub> with the smallest particles (ca. 80 nm), even after calcination at 500 °C. Our method afforded catalysts capable of a significantly higher rate of O<sub>2</sub> evolution under visible light than that of BiVO<sub>4</sub> catalysts prepared *via* conventional solid-state reactions, probably due to their smaller particle size and higher crystallinity. The present aqueous chelating method provides an environmentally benign process that can be used for the synthesis of highly active photocatalyst materials on a large scale without the use of toxic organic solvents.

## Acknowledgements

Assistant Professor Masanobu Higashi (Kyoto University) is acknowledged for the help in the apparent quantum efficiency measurements.

## Notes and references

<sup>a</sup> Research Institute, TOTO LTD., 2-8-1 Honson, Chigasaki-City, Kanagawa-pref. 253-8577, Japan. Fax: +81-467-54-1185; Tel: +81-467-54-3483; E-mail: hiromasa.tokudome@jp.toto.com

<sup>b</sup> Department of Energy and Hydrocarbon Chemistry, Graduate School of Engineering, Kyoto University, Katsura Nishikyo-ku, Kyoto 615-8510, Japan. Fax: +81-75-383-2478; Tel: +81-75-383-2478; E-mail: ryuabe@scl.kyoto-u.ac.jp

<sup>c</sup> Department of Molecular Chemistry and Biochemistry, Faculty of Science and Engineering, Doshisha University, 1-3 Tatara Miyakodani, Kyotanabe, Kyoto 610-0321, Japan.

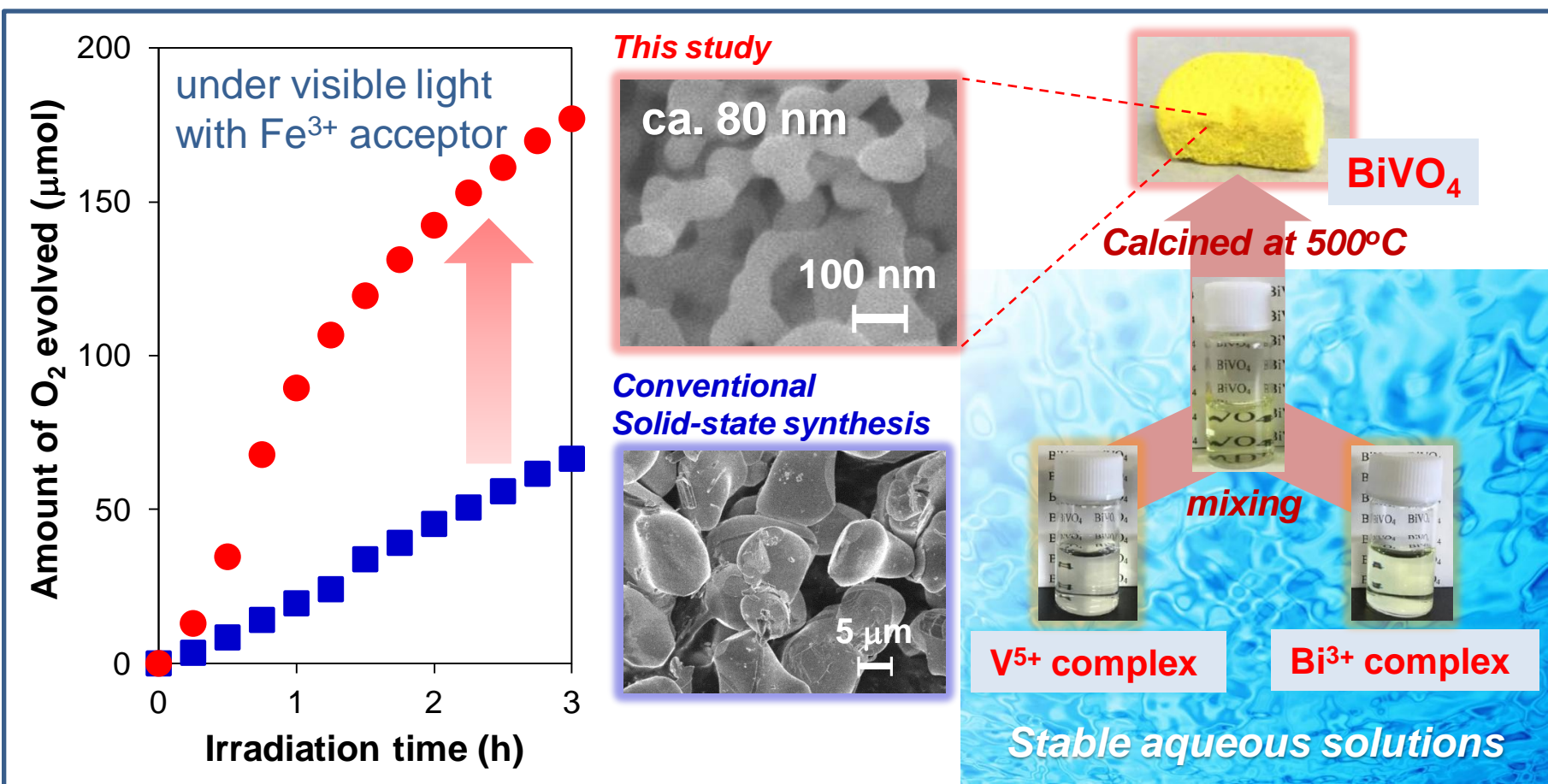
Electronic Supplementary Information (ESI) available: TG-DTA curves, Photographs, NMR, XRD patterns, SEM images data.

See DOI:10.1039/b000000x/

The authors have a patent application (JP2015-003840) on part of this work.

- 1 K. Maeda and K. Domen, *J. Phys. Chem. C*, 2007, **111**, 7851.
- 2 F. E. Osterloh, *Chem. Mater.*, 2008, **20**, 35–54.
- 3 A. Kudo and Y. Miseki, *Chem. Soc. Rev.*, 2009, **38**, 253–278
- 4 K. Maeda and K. Domen, *J. Phys. Chem. Lett.*, 2010, **1**, 2655–2661.
- 5 R. Abe, *J. Photochem. Photobiol. C: Photochem. Rev.*, 2010, **11**, 179–209.
- 6 A. Kudo, *Mater. Res. Bull.*, 2011, **36**, 32–38.
- 7 A. Fujishima and K. Honda, *Nature*, 1972, **238**, 37–38.
- 8 K. Maeda, K. Teramura, D. L. Lu, T. Takata, N. Saito, Y. Inoue and K. Domen, *Nature*, 2006, **440**, 295.
- 9 Y. Lee, H. Terashima, Y. Shimodaira, K. Teramura, M. Hara, H. Kobayashi, K. Domen, M. Yashima, *J. Phys. Chem. C*, 2007, **111**, 1042.
- 10 R. Asai, H. Nemoto, Q. Jia, K. Saito, A. Iwase and A. Kudo, *Chem. Commun.*, 2014, **50**, 2543–2546
- 11 C. Pan, T. Takata, M. Nakabayashi, T. Matsumoto, N. Shibata, Y. Ikuhara and K. Domen, *Angew. Chem.*, 2015, **127**, 2998–3002.
- 12 R. Abe, *Bull. Chem. Soc. Jpn.*, 2011, **84**, 1000–1030.
- 13 K. Maeda, *ACS Catal.*, 2013, **3**, 1486–1503.
- 14 K. Sayama, K. Mukasa, R. Abe, Y. Abe and H. Arakawa, *Chem. Commun.*, 2001, 2416–2417.
- 15 R. Abe, K. Sayama, K. Domen, H. Arakawa, *Chem. Phys. Lett.*, 2001, **344**, 339–344.
- 16 H. Kato, M. Hori, R. Kouta, Y. Shimodaira and A. Kudo, *Chem. Lett.*, 2004, **33**, 1348–1349.
- 17 H. Kato, Y. Sasaki, A. Iwase and A. Kudo, *Bull. Chem. Soc. Jpn.*, 2007, **80**, 2457–2464.
- 18 Y. Sasaki, A. Iwase, H. Kato and A. Kudo, *J. Catal.*, 2008, **259**, 133–137.
- 19 H. Kato, Y. Sasaki, N. Shirakura and A. Kudo, *J. Mater. Chem. A*, 2013, **1**, 12327–12333.
- 20 Y. Sasaki, H. Kato and A. Kudo, *J. Am. Chem. Soc.*, 2013, **135**, 5441.
- 21 A. R. Lim, S. H. Choh and M. S. Jang, *J. Phys.: Condens. Matter.*, 1995, **7**, 7309.
- 22 A. Kudo, K. Omori and H. Kato, *J. Am. Chem. Soc.*, 1999, **121**, 11459.
- 23 S. Tokunaga, H. Kato and A. Kudo, *Chem. Mater.*, 2001, **13**, 4624–4628.
- 24 B. Ohtani, O. Mahaney, F. Amano, N. Murakami and R. Abe, *J. Adv. Oxid. Technol.*, 2010, **13**, 247–261
- 25 R. S. Roth and J. L. Waring, *Am. Mineral.*, 1963, **48**, 1348.
- 26 A. W. Sleight, H. Y. Chen, A. Ferretti and D. E. Cox, *Mater. Res. Bull.*, 1979, **14**, 1571.
- 27 A. Kudo, K. Ueda, H. Kato and I. Mikami, *Catal. Lett.*, 1998, **53**, 229.
- 28 G. Li, D. Zhang and J. C. Yu, *Chem. Mater.*, 2008, **20**, 3983.
- 29 A. Iwase and A. Kudo, *J. Mater. Chem.*, 2010, **20**, 7536–7542.
- 30 A. Iwase, H. Kato and A. Kudo, *J. Sol. Energy Eng., B*, 2003, **104**, 36.
- 31 J. Yu and A. Kudo, *Chem. Lett.*, 2005, **34**, 850.
- 32 L. Zhang, D. Chen and X. Jial, *J. Phys. Chem. B*, 2006, **110**, 2668.
- 33 J. Yu and A. Kudo, *Adv. Funct. Mater.*, 2006, **16**, 2163–2169.
- 34 J. Yu, Y. Zhang and A. Kudo, *J. Solid State. Chem.*, 2009, **182**, 223–228.
- 35 S. Okunaka, H. Tokudome and R. Abe, *J. Mater. Chem. A*, 2015, **3**, 14794–14800.
- 36 S. Okunaka, H. Tokudome, Y. Hitomi and R. Abe, *J. Mater. Chem. A*, 2015, **3**, 1688–1695.
- 37 K. Zare, P. Lagrange and J. Lagrange, *J.C.S. Dalton.*, 1978, 1372–1376.
- 38 M. Bartušek and V. Šustáček, *Collection Czechoslovak Chem. Commun.*, 1983, **48**, 2785–2797.
- 39 M. M. Caldeira, M. L. Ramos, N. C. Oliveira and V. M. S. Gil, *Can. J. Chem.*, 1987, **65**, 2434–2440.
- 40 K. Popov, A. Vendilo and N. Djatlova, *Mag. Res. Chem.*, 1991, **29**, 301–303.
- 41 S. P. Summers, K. A. Aboud, S. R. Farrah and G. J. Palenik, *Inorg. Chem.*, 1994, **33**, 88–92.
- 42 Z. H. Zhou, H. Zhang, Y. Q. Jiang, D. H. Lin, H. L. Wan and K. R. Tsai, *Trans. Metal. Chem.*, 1999, **24**, 605–609.
- 43 M. Kaliva, C. P. Raptopoulou, A. Terzis and A. Salifoglou, *Inorg. Chem.*, 2004, **43**, 2895–2905.
- 44 A. R. Khan, D. C. Crans, R. Pauliukaite and E. Norkus, *J. Braz. Chem. Soc.*, 2006, **17**, 895–904.
- 45 P. Schwendt, A. S. Tracey, J. Tatiersky, J. Galikova and Z. Zak, *Inorg. Chem.*, 2007, **46**, 3971–3983.
- 46 L. R. Guilherme, A. C. Massabni, A. Cuin, L. A. A. Oliveira, E. E. Castellano, T. A. Heinrich and C. M. Costa-Neto, *J. Coord. Chem.*, 2009, **62**, 1561–1571.
- 47 J. Galikova, P. Schwendt, J. Tatiersky, A. S. Tracey and Z. Zak, *Inorg. Chem.*, 2009, **48**, 8423–8430.
- 48 Y. K. Kho, W. Y. Teoh, A. Iwase, L. Madler, A. Kudo and R. Amal, *ACS Appl. Mater. Interfaces.*, 2011, **3**, 1997–2004.
- 49 F. D. Hardcastle and I. E. Wachs, *J. Phys. Chem.* 1991, **95**, 5031–5041.
- 50 M. Kakihana, *J. Sol-Gel Sci Technol.*, 1996, **6**, 7–55.





Efficient photocatalytic O<sub>2</sub> evolution is demonstrated under visible-light on BiVO<sub>4</sub> fine particles prepared *via* newly developed aqueous chelating method.